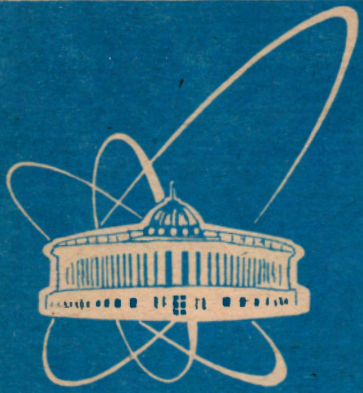

ОБЪЕДИНЕННЫЙ
ИНСТИТУТ
ЯДЕРНЫХ
ИССЛЕДОВАНИЙ

Дубна

E15-96-207

D.L.Demin, A.E.Drebushko, V.P.Dzhelepov, V.V.Filchenkov, N.N.Grafov, V.G.Grebinnik, D.V.Migachev, A.D.Konin, A.I.Rudenko, V.T.Sidorov, Yu.G.Zhestkov, V.G.Zinov, J.D.Davies[1], V.R.Bom[2], C.W.E. van Eijk[2]

MEASUREMENT OF THE SPIN AND TEMPERATURE DEPENDENCE OF THE *dd*μ-MOLECULE FORMATION RATE IN SOLID AND LIQUID DEUTERIUM

Submitted to «ЖЭТФ»

[1]University of Birmingham, Edgbaston, Birmingham B15 2TT, U.K
[2]Delft University of Technology, NL-2629 JB, Delft, Netherlands

1996

1 Introduction

Muon catalyzed fusion (MCF) in pure deuterium (see scheme in fig. 1), has relatively simple kinetics and so is an attractive way to check the basic principles of the theory of muonic molecule resonance formation. Recent years have provided significant success both in the theoretical consideration [1], [2], [3] of and in the measurements [4], [5], [6] of the $dd\mu$-molecule formation rate ($\lambda_{dd\mu}$) including strong spin effects. As is seen from fig. 2, measurements of the temperature dependence $\lambda_{dd\mu}(T)$ at $T > 20\ K$ are in excellent agreement with the "standard" theory of resonance muonic molecule formation. The most impressive consequence of their comparison is the determination of the energy of the weakly bound level in the $dd\mu$-system with an accuracy $\simeq 0.1\, meV$. Note that the latter corresponds to 1% of the relativistic contributions to this energy.

It was thought that measurements at lower temperatures would allow only improved accuracy of the main MCF parameters. However, the recent measurement of the $dd\mu$-molecule formation rate from the spin F=3/2 state of the $d\mu$-atom at T=3K [7] shows a large discrepancy with theory. Our aim was to extend the systematic measurement of $dd\mu$ mesomolecule formation rate from the different hyperfine, $d\mu$-atom states $\lambda_{3/2}$ and $\lambda_{1/2}$ and the hyperfine transition rate λ_d within the 5–30 K temperature range. Preliminary results have been published [8].

In this paper we give the results of full analysis including the determination of the absolute values both resonant (from the $d\mu$-atom spin state $F = 3/2$) and nonresonant ($F = 1/2$) $dd\mu$-molecule formation rates. At low deuterium temperature these values were previously measured in liquid deuterium at T=22 K [6] and T=23 K [4] and showed

a noticeable discrepancy with theory for the value of $\lambda_{1/2}$ (nonresonant) [9]. For normalization the authors of [7] used the value of $\lambda_{1/2}$ obtained in [4] and then corrected in [10]; also they were not able to measure the deuterium density directly in the experiment.

The important features of the present work are the measurements with liquid and solid deuterium were performed in the same experiment under conditions having well defined deuterium density and temperature.

2 Experimental method

The experimental method has been detailed elsewhere [6]. We measured and analyzed the yield and time distribution of 2.5 MeV neutrons from the d+d fusion reaction at seven temperatures in the range 5-30K

$$d\mu + d \longrightarrow dd\mu \longrightarrow {}^3He + n \qquad (1)$$

A simplified schematic of the experimental apparatus is shown in fig. 3, in particular a specially constructed solid deuterium target (T) of volume 280 cm^3 [11] and a total absorption neutron spectrometer [12] (NE-213 to provide $n-\gamma$ separation [13]). The spectrometer consisted of two identical parts symmetrically placed around the target with total volume 22 l. High neutron detection efficiency (solid angle $\simeq 65\%$ and intrinsic efficiency $\simeq 70\%$ resulted in sufficient counting rate yet relatively low accidental background.

The target was enclosed in a liquid helium cooling cryostat. Special attention was paid to achieving high uniformity in temperature and density throughout the large target volume. To this end a heat conductor consisting of 500 copper wires 0.4 mm in diameter was set inside the target resulting in temperature gradients throughout the target not higher than 0.1 K. Temperatures were measured by two helium thermometers placed at different heights within the target and were kept constant to within an accuracy of 0.2 K.

The deuterium was purified with a palladium filter down to $10^{-1} ppm$ impurity concentration. The protium content was not higher than 0.5%.

The trigger selected those events for further recording and analysis which corresponded to the appearance of the neutron ($\bar{4}$.(N1+N2)) and electron (4.(N1+N2)) signals during the 10 μs gate, opened by the muon stop (1.2.3.$\bar{4}$) signal. Discriminating against backgrounds originating from muon stops in the target walls place the requirement on electron times of $t_e > 0.2\,\mu s$ after the muon stop ($t_0 = 0$).

As usual, the neutron yield was normalized to the number of electrons from the decay of muons stopped in deuterium. The time spectrum of μ–decay electrons was obtained in the run at 19.0 K is shown in fig. 4. It was analyzed using the expression

$$N(t) = a_1 \cdot exp(-\lambda \cdot t) + a_2 \cdot v(t) + a_3 \qquad (2)$$

Here the short-lived component $a_2 \cdot v(t)$ (dashed curve in the fig. 3) represents muon stops in the target walls; its form was determined from the measurements with an empty target. The slow exponent corresponds to muons stopped in deuterium with slope very close to the free muon disappearance rate $\lambda_0 = 0.455\,\mu s^{-1}$. The number of events belonging to the slow component (N_e) was used in analysis of neutron events.

Experimental conditions for the 9 full runs are given in Table 1. As usual, density is normalized relative to that of liquid hydrogen (LHD, $\phi_0 = 4.25 \cdot 10^{22}\, nuclei/cm^3$). Numbers in brackets represent uncertainties in the last figure(s).

Table 1. Parameters of exposures.

Number	Target filling	Temperature, K	Density (LHD)	$N_e\,(10^6)$
1	Deuterium, solid	5.5(3)	1.43(4)	4.49(18)
2	—"— —"—	9.9(2)	1.43(4)	2.983(14)
3	—"— —"—	15.1(2)	1.42(4)	2.842(14)
4	—"— —"—	17.7(2)	1.40(4)	5.777(19)
5	Deuterium, liquid	19.0(2)	1.31(4)	4.598(17)
6	—"— —"—	26.3(3)	1.19(4)	2.786(13)
7	—"— —"—	30.5(3)	1.08(4)	1.738(12)
8	Helium	14.7(2)	0.37(1)	1.487(9)
9	Vacuum			

The highest statistics were accumulated at the lowest temperature and in runs 4.5 which were as close as possible in temperature but in different deuterium phase states. The measurement with helium was made to determine independently the neutron background (a_3 in equation 2 above) while the data obtained with an empty target allowed us to check the number of muon stops in the target walls.

Those events were selected for further analysis which satisfied the criteria of having:
1) a neutron in the $n-\gamma$-plot [6], [12];
2) a μ-decay electron in the time interval $t_n + 0.5\,\mu s \le t_e \le t_n + 2.5\,\mu s$.
Times and amplitudes (recoil proton energy) for those events were accumulated separately for each run and neutron detector. The final results were obtained from the analysis of such distributions for the "first detected" neutron events. However the high neutron detection efficiency allowed us to register the "second detected" fusion neutron; their yield and time distributions were then used to verify both the normalization procedure and the detection efficiency calculation. Some neutrons time distributions are presented in figs 5a, 5b and 6. One can see that the relative yield of the background is low and that the neutron spectrum behavior remains the same when the temperature and the phase state of deuterium are changed.

3 Kinetics of the d-d fusion cycle

The scheme of the $d+d$ muon-catalyzed processes in pure deuterium is shown in Fig. 1. According to "standard" theory [1], [2] $d\mu$-atoms are formed with an initial kinetic energy of a few eV in two hyperfine states from which they are quickly thermalized. The thermalization rate is estimated to be $\lambda_{therm} \sim 10^9 \cdot \phi\, s^{-1}$ [14], [15] which is much higher than the μ-molecule formation and spin-flip rates. Therefore the thermalization stage is neglected in the"standard" theory.

Muonic molecules can be formed either via the nonresonant Auger process where the energy released under $dd\mu$-formation is transferred to the conversion electron or via the Vesman resonance mechanism [16]. The rate of non-resonant $dd\mu$-molecule formation depends slightly on the $d\mu$-atom energy ($\epsilon_{d\mu}$) and is equal to $0.03 - 0.04\,\mu s^{-1}$ at $T \le 50\,K$ [9]. According to the Vesman scheme the resonant $dd\mu$ formation proceeds *via* the complex $[(dd\mu), d, 2e]^*$ which is in an exited state. This process is characterized by a set of resonances whose positions are determined by the spin states of the $d\mu$-atom ($F = 3/2,\ 1/2$) and of the $dd\mu$- molecules ($S = 3/2,\ 1/2$) as well as by the rotation states

of the "initial" D_2- molecule(K_i) and the complex (K_f). Taken from calculation [17] the most intensive resonances are shown in fig. 8. The transitions having

$$F = 3/2 \longrightarrow S = 1/2, \;\; K_i = 0 \longrightarrow K_f = 1, \;\; K_i = 1 \longrightarrow K_f = 2 \qquad (3)$$

dominate at the lowest temperatures.

Normally $dd\mu$ formation is neglected during thermalization but is considered for the Maxwell distributions of the $d\mu$-atom thermal energies. So, to obtain the values of $\lambda_{dd\mu}(T)$ for a given temperature, one integrates the function $\lambda_{dd\mu}(\epsilon_{d\mu})$ over the Maxwellian $W(\epsilon_{d\mu};T)$. This procedure was used in [18] to give the theoretical dependence of $\lambda_{3/2}(T)$ presented in fig. 2. Maxwell distributions for T=5K and 20K are shown in fig. 8 together with the resonance closest in energy. As can be seen from this figure, the thermal energy distribution for T=5 K does not overlap with this resonance. So only the non-resonant $dd\mu$-formation is expected to contribute at this temperature. From fig. 8 it follows also that at T=20 K $d\mu$-atoms spend a small part of their "Maxwell cycle" in the resonance region.

So we conclude that the measured value of $\lambda_{dd\mu}$ should be compared with a calculated "effective" value which includes:
1) a contribution during the thermalization stage, not higher than a few percent [1] [2]
2) integration over the Maxwell distribution. Note that competition between spin-flip and scattering processes was not taken into account (see [18]);
3) only $\simeq 1/4$ part of $dd\mu$-molecules undergoes fusion in competition with the back decay of the complex [1].

4 Analysis

A set of differential equations corresponds to the scheme of the $d-d$ fusion cycle shown in fig. 1. When thermalization and $d+d$ fusion rates are sufficiently high it has an exact solution [1] which gives for the form of the neutron time distribution [1], [19] :

$$F_n(t) = b_f \cdot exp(-\lambda_f \cdot t) + b_s \cdot exp(-\lambda_s \cdot t). \qquad (4)$$

For the *fast* exponent its slope λ_f is determined mainly by the spin-flip rate λ_d and its amplitude b_f by the value of $\lambda_{3/2}$. The amplitude of the *slow* component b_s is close to the value of $\lambda_{1/2}$.

The parameters of the function (4) were found from the fit of the time distributions of the "first detected" neutrons. These spectra were convoluted with a gaussian resolution function to account the finite time resolution (σ). The value of σ as well as the time zero (t_0) were optimized for each run. The analysis showed that the time zero stability during the data-taking was better than $1\,ns$. Background due to muon stops in the target walls was approximated by an exponent with the slope ${\lambda_f}^b = 5\,\mu s^{-1}$. Accidental neutron events were fitted as an exponent with ${\lambda_s}^b = \lambda_0$ for $t_n \geq t_0$ and with a constant value for $t_n \leq t_0$.

At the next stage of the analysis the absolute values of the *steady state* $dd\mu$-molecule formation rate were obtained from

$$\lambda_{ss} = \lambda_s \cdot [{N_n}^s / N_e \cdot \epsilon_n \cdot f_t] / \phi \cdot \beta_s \qquad (5)$$

Here the expression in the square brackets means the absolute neutron yield for the *steady state* of the d-d fusion cycle, λ_s is slope of the "slow" exponent in (4) and β_s is the partial

probability of the reaction (1). To good approximation (better than 1%) $\beta_s = \beta_{nr} = 0.53$, where β_{nr} corresponds to the nonresonant $dd\mu$-formation.

In the expression for the absolute neutron yield ${N_n}^s$ is the number of neutron events in the "slow" component of the time spectrum (4), N_e is the number of electrons indicated in table 1, f_t allows for the finite time interval for detection of a fusion neutron followed by a μ-decay electron and ϵ_n is the neutron detection efficiency. The latter was calculated using two "independent" Monte-Carlo codes. One [20] was written specially for our experimental $d-d$ program and the other used the standard package GEANT [21] and the low energy neutron cross sections therein. The results of two codes coincide with an accuracy $3-5\%$. To determine the efficiency loss due to the finite threshold the calculated recoil proton energy spectrum was reconciled with the experimental distribution. This procedure was repeated for data of each run and the example for T=19.0 K is given in fig. 9. Spikes in the spectrum are due to ADC differential nonlinearity.

The value of λ_{ss}, as well as the slope λ_s and the ratio b_f/b_s (eq. 4), are found from the fit used for the numerical solution of the set of differential equations referred to above. For the partial probability of reaction (1) $\beta_r = 0.58$ was used for the resonance $dd\mu$ formation ($F = 3/2$) and $\beta_{nr} = 0.53$ for the non-resonant one ($F = 1/2$) [22]. This procedure then gave the values of $\lambda_{3/2}$, $\lambda_{1/2}$ and λ_d. There were a few small corrections (a few $\sim$) e.g. for the loss due to $n-\gamma$ separation.

5 Results and discussion

The experimental results are presented in table 2.

Table 2. Experimental results.

Temperature, K	The rates of the $dd\mu$-molecule formation and $d\mu$-atom hyperfine transition rate (μs^{-1})			
	$\lambda_{1/2}$	$\lambda_{3/2}$	$\lambda_{3/2}/\ \lambda_{1/2}$	λ_d
5.5	0.0448(18)	2.48(13)	55.3(18)	31.7(10)
9.9	0.0403(20)	2.11(14)	52.3(23)	29.3(12)
15.1	0.0424(20)	2.27(16)	53.5(24)	32.5(15)
17.7	0.0419(18)	2.24(11)	53.4(17)	32.8(12)
19.0	0.0407(21)	2.27(14)	55.8(19)	30.2(10)
26.3	0.0389(20)	3.03(20)	77.8(24)	36.1(14)
30.5	0.0428(26)	3.20(21)	74.8(24)	32.0(11)

The values in brackets are the errors due only to statistics, fit and corrections and do not include systematic uncertainties from ϕ (3%) and ϵ_n (8%). Our results are shown in figures 2 and 10 together with the data of other authors. Again our data are given without systematic errors to show more clearly their dependence on temperature.

The data for the "second detected" neutrons (N1-N2 and N2-N1) were also analyzed. Their time distribution relative to the "first detected" neutrons is shown in fig. 7. The data are summed over all exposures with solid deuterium. The curve in this figure corresponds to exponents with the "fast" and "slow" slopes found above in the analysis of the "first" neutrons. There is satisfactory agreement of measured and predicted spectra.

The value of ${\lambda_{1/2}}^{(2)}$ was found from the analysis of the "second" neutrons normalized

on the number of "first" neutrons, viz

$$\lambda_{1/2}{}^{(2)} = 0.041(3)\,\mu s^{-1} \qquad \text{(statistical error only)}$$

This agrees with that obtained for the "first" neutrons.

As can be seen from fig. 2 our data for $\lambda_{1/2}$ are in an agreement both with our previous measurement with liquid deuterium at $T = 22\,K$ and with the results of the PSI group at $T = 23\,K$; the latter initially gave $\lambda_{1/2} = 0.0500(34)(22)\,\mu s^{-1}$ [4] and then in [10] as $\lambda_{1/2} = 0.045(5)\,\mu s^{-1}$. Also the experimental results are in excess of theoretical prediction, $\lambda_{1/2}(\text{th}) \sim 0.03$ [9].

Of course, our main result is the measurements of the $dd\mu$-molecule formation rate from the upper $d\mu$-atom spin state for the lowest deuterium temperatures. Together with the pioneering result of the TRIUMF group [7] they sharply contradict the "standard" theory according to which only the non-resonant $dd\mu$ formation from both $d\mu$-atom spin states can contribute at the lowest temperatures. Possible mechanisms to explain it are considered in [18], [22], [23].

According to [22] $d\mu$-atoms moving in solid deuterium have insufficient time to fully thermalize because they lose energy only in inelastic interactions with the lattice excitation. So, significant $dd\mu$ formation occurs at energies higher than thermal ones. This effect can explain the experimental data qualitatively [18] but quantitative agreement with experiment is achieved only for some definite values of the inelastic cross sections. This mechanism could be investigated by repeating the experiment with enhanced protium.

Another possible explanation involves transitions with negative $d\mu$-atom resonance energy for $dd\mu$ formation [23] with the transfer of the released energy to lattice excitation. The transition $K_i = 1 \longrightarrow K_f = 0$ is appropriate for this scheme. Now the liquid and solid deuterium in this experiment had the room temperature, ortho-para ratio because equilibration is so slow. The experiment should be repeated with catalysed $p \longrightarrow \sigma$ to, inter alia, check this mechanism because with pure ortho-deuterium [23] only transitions with positive resonance energies are possible - (3) above.

Of course, both mechanisms can explain the experimental results, but as was pointed out in [18], the data for solid and liquid deuterium are practically identical. Perhaps the problem is more complicated and needs a more complete consideration. Incidentally the enhanced rate is independent of the structure of the solid deuterium lattice viz the TRIUMF group formed fcc solid deuterium directly from the gas phase whereas our solid deuterium had hcp structure as it came from the liquid.

Finally, the experimental data on λ_d are given in fig. 10. Our results are in an agreement with previous measurements both in solid and liquid deuterium. At the same time full set of the data for $T \leq 30\,K$ does not show such sharp difference with the results for gaseous deuterium as was manifested for the first measurement in liquid deuterium.

Acknowledgments

The authors thank E.P. Krasnoperov for developing the solid deuterium target, and M.M. Petrovsky' and A.P. Kustov for the help in tests and runs.

The work is performed under the assistance of the Russian Foundation for Basic Research and INTAS (Brussels).

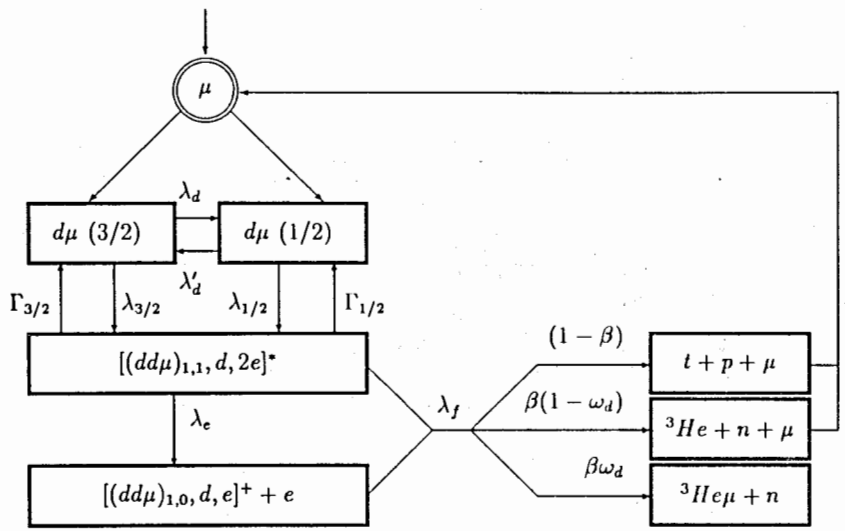

Figure 1. **Scheme of μ – catalyzed processes in pure deuterium.**

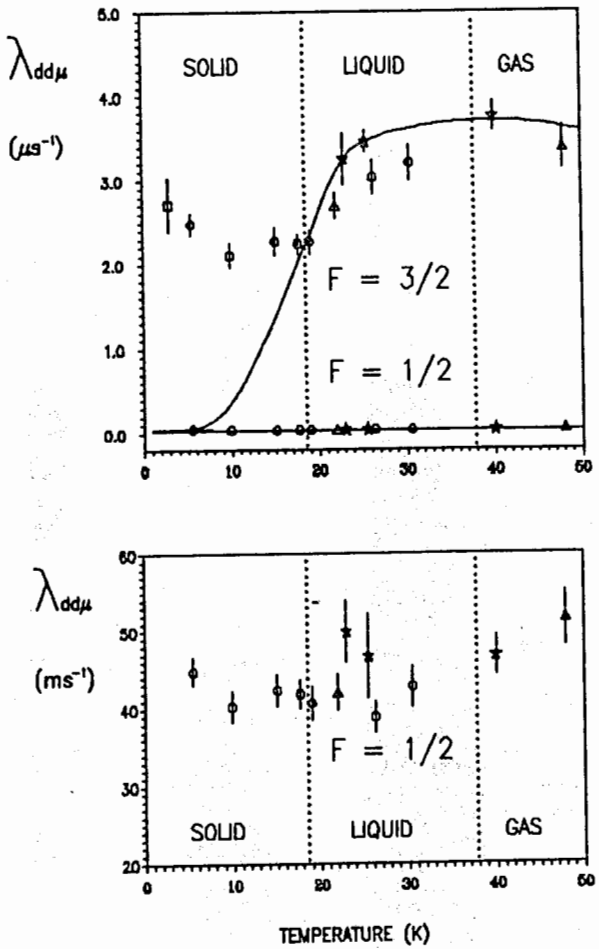

Figure 2. **Dependence** $\lambda_{dd\mu}(T)$. Square– [7]; circles– present work; triangles– previous Dubna measurements [6]; stars– [4], [5]. The line corresponds to the "standard" theory [1-3].

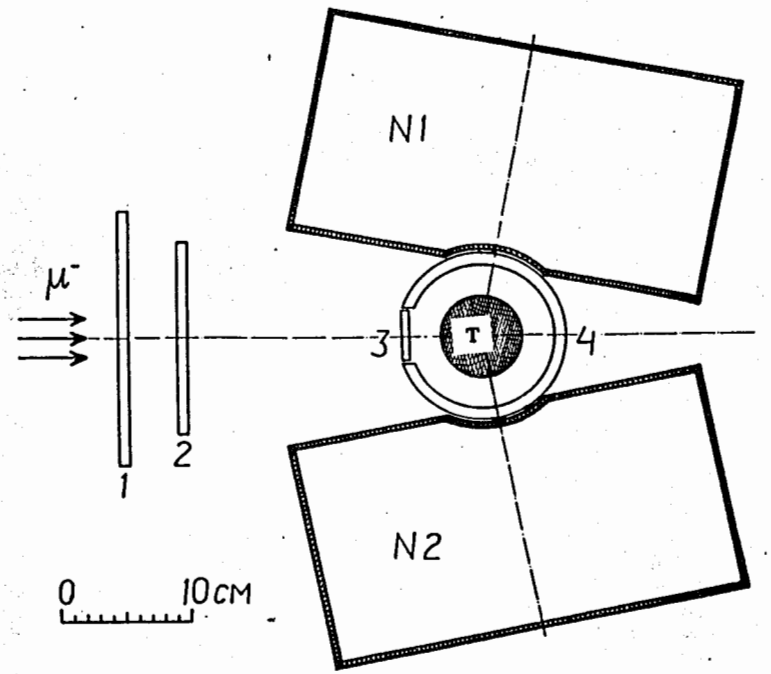

Figure 3. **Simplified schematic of the experimental setup.** 1,2,3,4 are scintillation counters; N1,N2 are total absorption neutron detectors, T is the deuterium target.

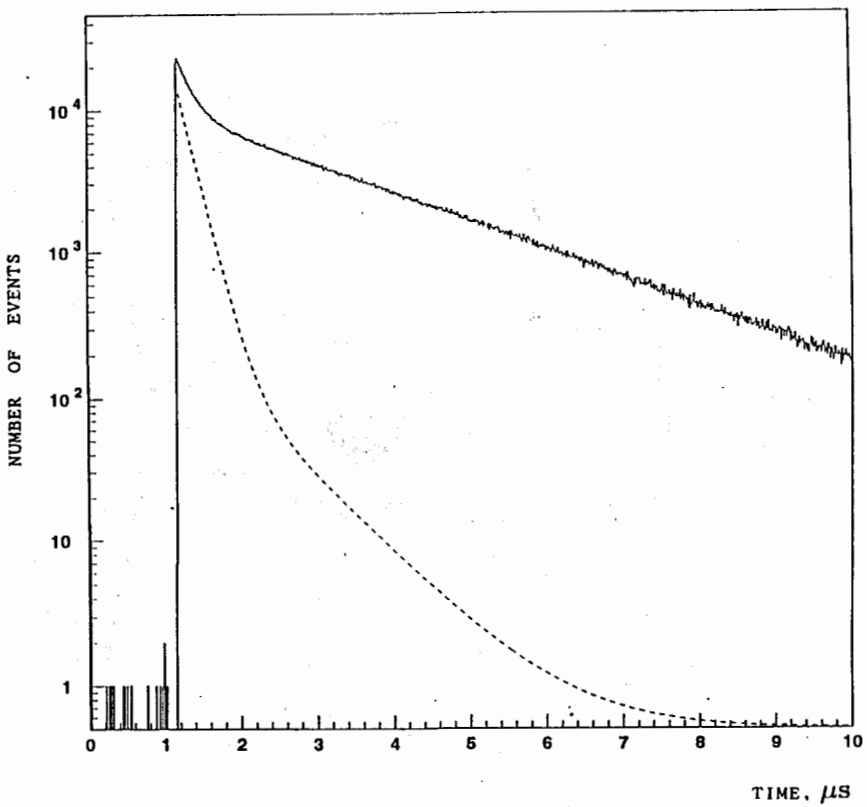

Figure 4. **Time spectrum of decay electrons.** The dashed line represents muon stops in the target walls.

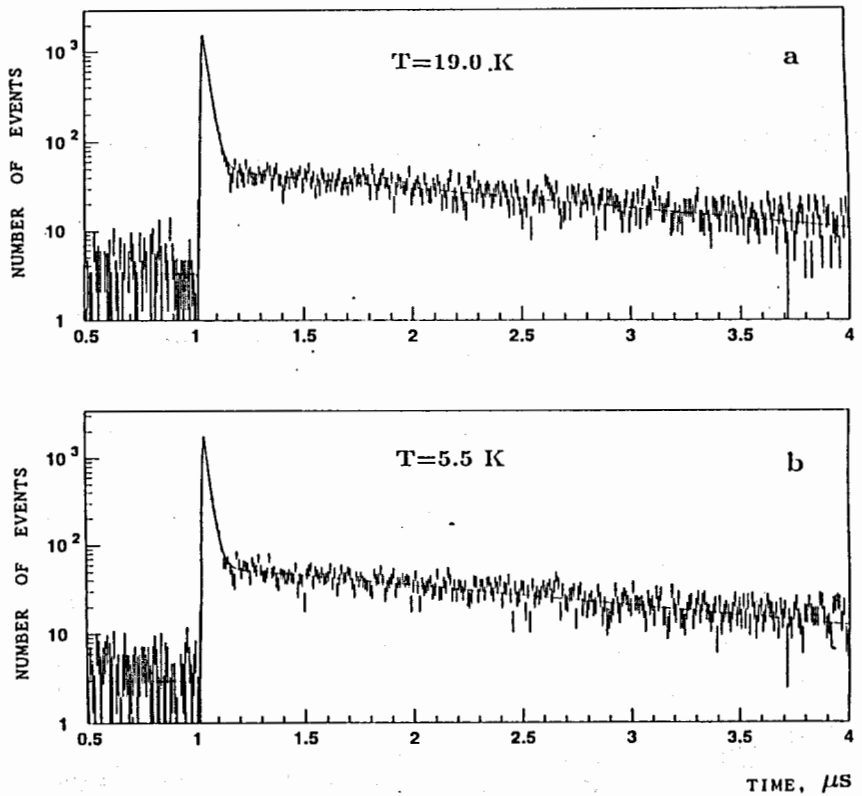

Figure 5. **Time spectra of the "first detected" catalysis neutron.** The deuterium temperature: a 19.0 K (liquid); b 5.5 K (solid). Lines correspond to the function (4) with an optimal parameters found from the fit.

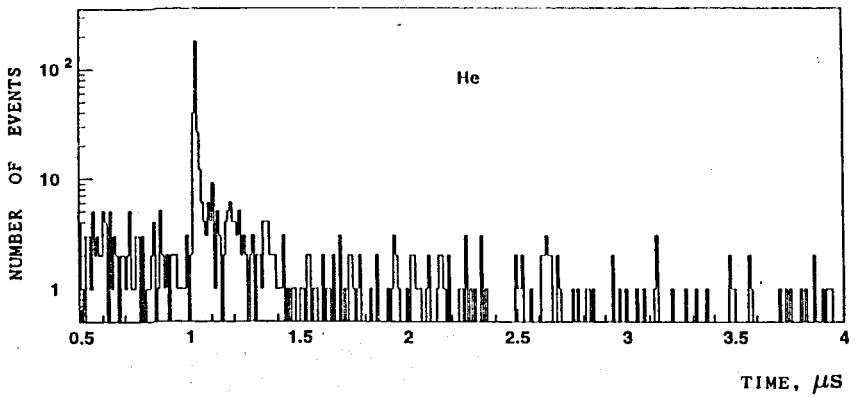

Figure 6. **Time spectrum of background neutron events** (target is filled with helium).

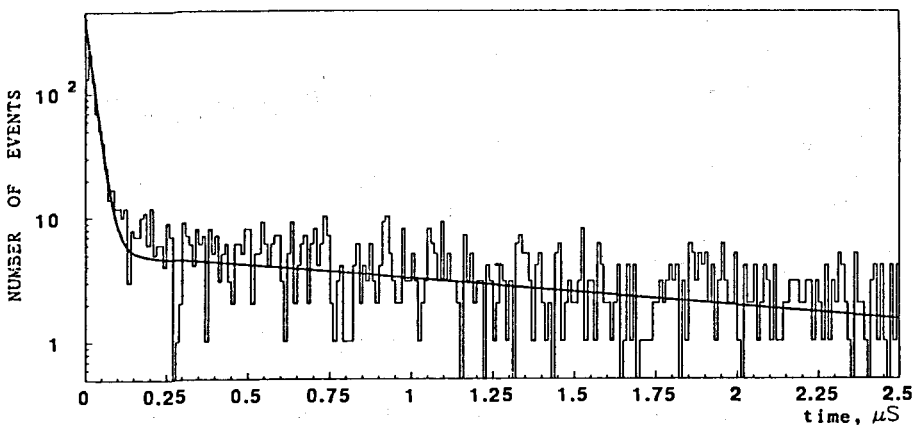

Figure 7. **Time distribution of the "second detected" neutron accumulated for all exposures with solid deuterium.** Line is the function (4) with the exponent slopes obtained from the analysis of the first detected neutrons.

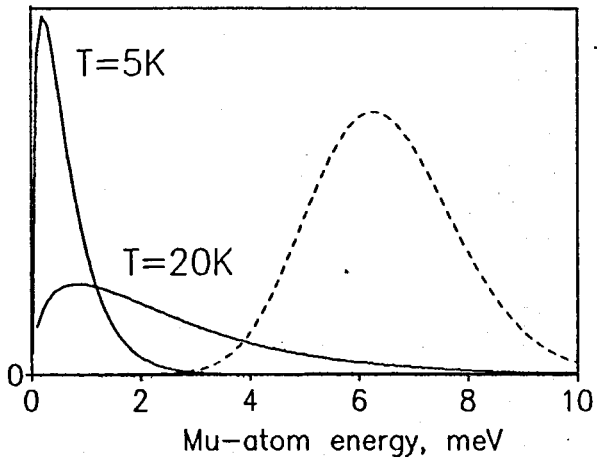

Figure 8 **Maxwell energy distribution of $d\mu$-atoms for T=5 K and T=20 K.** The closest to zero resonance in the $dd\mu$-formation is shown by the dashed line.

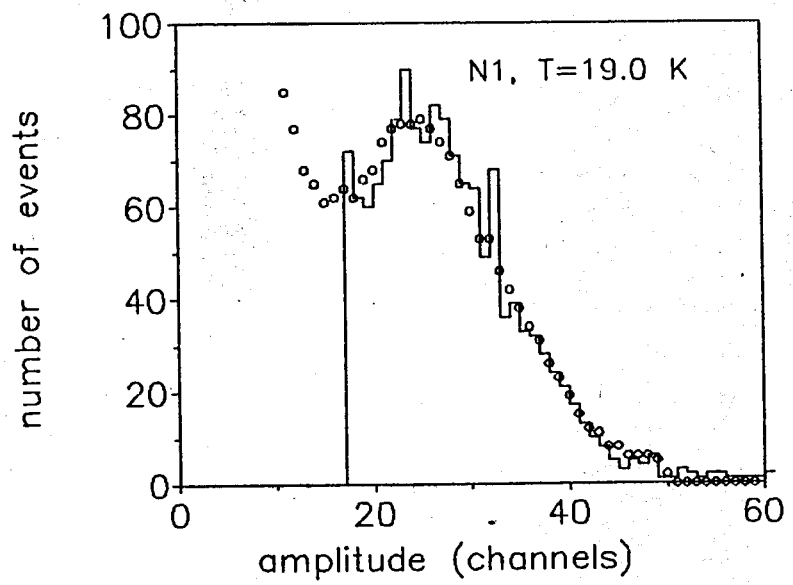

Figure 9. **Energy spectrum of protons recoiling from neutrons plotted for detector N1 with the target at 19.0 K (histogram).** Circles are the corresponding calculations. Number of events are given in arbitrary units.

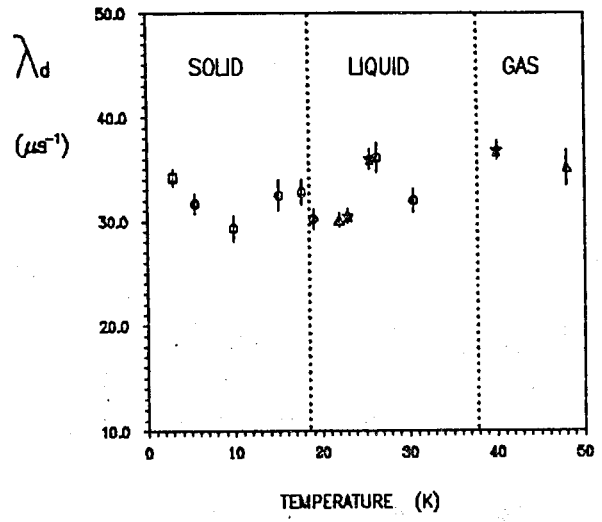

Figure 10. **Experimental data on the $d\mu$-atom spin-flip rate,** λ_d Square– [7]; circles– present work; triangles– previous Dubna measurements [6]; stars– [4], [5].

References

[1] L.I. Menshikov, L.I. Ponomarev, T.A. Strizh, M.P. Faifman, Zh.Exp.Theor.Phys. **92**, 1173 (1987), *Sov. Phys. - JETP* **65**, *656 (1987).*

[2] M.P. Faifman, Muon Cat. Fusion **2**, 247 (1988). M.P. Faifman, L.I. Menshikov, T.A. Strizh, Muon Cat. Fusion **4**, 1 (1989).

[3] A. Zcrinzi, Muon Cat. Fusion **5/6**, 179 (1990).

[4] N. Nagele, W.H. Breunlich, M. Cargnelli et al., Nucl. Phys. A, **493**, 397 (1989).

[5] J. Zmescal, W.H. Breunlich, M. Cargnelli et al., Muon Cat. Fusion **1**, 109 (1987). W.H. Breunlich, M. Cargnelli, P. Kammel et al., Muon Cat. Fusion **5/6**, 149 (1987).

[6] V.P. Dzhelepov, V.G. Zinov, S.A. Ivanovsky' et al., Zh. Exp. Teor. Phys. **101**, 1105 (1992), *Sov. Phys. - JETP* **74**, *589 (1992)*, *Muon Cat. Fusion* **7**, *387 (1992).*

[7] P. Kammel, in *Muonic Atoms and Molecules*, Proc. of the Int. Workshop at the Centro Stefano Franchini on Monte Verita, ed. by L. Schaller and C. Petitjean, Birkhauser Verlag, CH-4010, Basel, Boston, Berlin, 111 (1993). P.E. Knowles, J.M. Bailey, G.A. Beer et al., Hyp. Int. (1996).

[8] D.L. Demin, V.P. Dzhelepov, V.V. Filchenkov et al., Hyp. Int. (1996).

[9] M.P. Faifman, Muon Cat. Fusion, **4**, 341 (1989), *Hyp. Int. (1996).*

[10] A. Scrinzi, P. Kammel, J. Zmeskal et al., Phys. Rev. A, **47**, 4691 (1993).

[11] D.L. Demin, V.P. Dzhelepov, N.N. Grafov et al., Hyp. Int. (1996).

[12] V.P. Dzhelepov, V.V. Filchenkov, A.D. Konin et al., Nucl. Instr. and Meth. A, **269**, 634 (1988).

[13] V.G. Zinov, E. Lonsky, A.I. Rudenko, Prib. Tech. Exp. **1**, 91 (1991).

[14] A. Adamchak, V.S. Melezhik, Muon Cat. Fusion **5/6**, 303 (1990).

[15] J.B. Kraiman, W.H. Breunlich, M. Cargnelli et al., Muon Cat. Fusion **5/6**, 43 (1990), *Phys. Rev. Lett.* **63**, *1942 (1989).*

[16] E.A. Vesman, Pis'ma Zh. Exp. Teor. Phys. **5**, 113 (1967), (*Sov. Phys. - JETP Letters* **5**, *91 (1967)*).

[17] M.P. Faifman, Hyp. Int. (1996).

[18] V.V. Filchenkov, Hyp. Int. (1996).

[19] V.V. Filchenkov, Communications JINR E1-89-57, Dubna (1989).

[20] V.V. Filchenkov, L. Marczis, Communications JINR E13-88-56, Dubna (1988).

[21] CERN, Program Library, **W5013**.

[22] A. Adamchak, Hyp. Int. (1996).

[23] V.V.Filchenkov, L.I.Men'shikov, Hyp. Int. (1996).

Received by Publishing Department
on June 13, 1996.

Демин Д.Л. и др. E15-96-207

Измерение спиновой и температурной зависимости скорости образования молекулы $dd\mu$ в твердом и жидком дейтерии

Измерена скорость образования молекулы $dd\mu$ из двух состояний сверхтонкой структуры $d\mu$-атома в диапазоне температур $T = 5 — 30$ K. Результаты сопоставимы с измерениями группы TRIUMF при $T = 3$ K и противоречат предсказаниям теории. Работа выполнена на фазотроне ЛЯП ОИЯИ (Дубна).

Работа выполнена в Лаборатории ядерных проблем ОИЯИ.

Препринт Объединенного института ядерных исследований. Дубна, 1996

Demin D.L. et al. E15-96-207

Measurement of the Spin and Temperature Dependence of the $dd\mu$-Molecule Formation Rate in Solid and Liquid Deuterium

$dd\mu$ molecule formation rates have been measured from the two hyperfine states of the $d\mu$-atom in the temperature range of $T = 5 — 30$ K. Results are consistent with the measurement of the TRIUMF group at $T = 3$ K and contradict theoretical predictions. The work was performed on the JINR phasotron (Dubna).

The investigation has been performed at the Laboratory of Nuclear Problems, JINR.

Preprint of the Joint Institute for Nuclear Research. Dubna, 1996